Electroactive Polymers and Macromolecular Electronics

CHRISTOPHER E. D. CHIDSEY AND ROYCE W. MURRAY

Electrodes can be coated with electrochemically reactive polymers in several microstructural formats called sandwich, array, bilayer, micro-, and ion-gate electrodes. These microstructures can be used to study the transport of electrons and ions through the polymers as a function of the polymer oxidation state, which is essential for understanding the conductivity properties of these new chemical materials. The microstructures also exhibit potentially useful electrical and optical responses, including current rectification, charge storage and amplification, electron-hole pair separation, and gates for ion flow.

ELECTRON-TRANSFER ACTIVE (ELECTROACTIVE) POLYMERS represent an emerging class of important conductive materials (*1, 2*). In the first part of this article we discuss how fundamental studies of these conductive materials can be aided by fabricating miniaturized structures (microstructures) from them. A significant benefit of the miniaturization is shortening of the distances over which ions and electrons must move in films of the polymers for their electrical, ionic, and other chemical properties to be measured. In the second part of the article, we introduce some possible technological applications of microstructures built from these polymers. Although the microstructures that have already been made are of impressively small dimensions (from 5 nm to 10 μm), they are neither numerous nor highly sophisticated. Thus they should be viewed as pioneer structures that may in the future lead to useful macromolecular electronic devices.

Electroactive polymers fall into three broad categories: π-conjugated, electronically conducting polymers (Fig. 1, A and B); polymers with covalently linked redox groups (redox polymers, Fig. 1, C and D); and ion-exchange polymers (Fig. 1, E and F). Features that such polymers have in common are semirigid mechanical properties, the ability to pass electrical current, and the ability to be oxidized or reduced by electrolysis. Electroactive polymers are ordinarily used as films in contact with electrodes, which serve as connectors for the electron flow and provide the electrical potential driving force for the oxidation state changes.

The π-conjugated materials, for example polyacetylene and polypyrrole (Fig. 1), have relatively delocalized electronic states, are electronically conducting, and are sometimes called organic metals. The conductive states are made by oxidative or reductive doping with chemical reagents such as oxygen (*3*), the halogens (*4*), and arsenic pentafluoride (*5*) or electrochemically by partial oxidation or reduction in contact with an electrolyte solution (*6, 7*). Redox polymers (*8, 9*) and ion-exchange polymers loaded with electroactive counterions (*10*) are localized state conductors (Fig. 1) and are less highly conducting than the π-conjugated materials. Redox polymers conduct current by electron self-exchange reactions (hopping) between neighbor redox sites, and ion-exchange polymers conduct by both electron self-exchange reactions and by physical diffusion of the electroactive counterions.

The film-making step is an important aspect of successfully fabricating microstructures from electroactive polymers. Films have been formed in many ways (*1*), including casting from solutions of the polymer or of reactive monomers (typically organosilanes), grafting of redox sites onto already formed polymer films, ion exchanging into ion-exchange polymer films, and electrochemical polymerization from monomer solutions. Electrochemical polymerization has been a particularly effective method for microstructuring, and the polypyrrole and poly[Os(bpy)$_2$(vpy)$_2$](ClO$_4$)$_2$ films of Fig. 1 are made in this way (*6, 8*).

Electroactive polymer films are interesting to electrochemists because they can be used to store electrical charge or as catalysts in electrochemical reactions. Both require the presence of mobile ionic species (counterions) to maintain electroneutrality in the electroactive polymer as it is oxidized or reduced. For example, during oxidation of a film of poly[Os(bpy)$_2$(vpy)$_2$](ClO$_4$)$_2$, additional anions will migrate into the film from a contacting electrolyte solution as shown in reaction 1.

$$\text{poly}[\text{Os(bpy)}_2(\text{vpy})_2](\text{ClO}_4)_2 + \text{ClO}_4^- \rightarrow \text{poly}[\text{Os(bpy)}_2(\text{vpy})_2](\text{ClO}_4)_3 + e^- \qquad (1)$$

As another example, reducing the conducting, polycationic form of polypyrrole produces a more neutral material, and the excess anionic counterions egress into the solution. The necessity for such ion motion events has a strong bearing on the proper design of electroactive polymer microstructures.

Electroactive polymers have characteristics similar to two classical components of electrochemistry: dense, highly conducting metal electrodes and small, freely diffusing ions and molecules in electrolyte solutions. Somewhat like metallic electrodes, electroactive polymers can conduct electrons and have some mechanical rigidity; that is, structures can be built from them, thin films can be formed and can act as mechanical barriers between phases, and small spots and strips of polymers can be made and retain their shape. But unlike solid metals and more like solutions, electroactive polymers are dynamic matrices in that their interiors can have variable compositions. Counterions move in them, as indicated above. Other species such as solvent molecules or other solutes may have significant long-range mobility, while redox groups such as the pendant ferrocene sites in polyvinylferrocene (Fig. 1) may only move over a few nanometers before being restrained by the polymer backbone.

Clearly, transport of electrons and ions through electroactive polymers is an important topic. The study of transport has been both a significant part of research on polymer-coated electrodes and

---

C. E. D. Chidsey is a member of the technical staff of AT&T Bell Laboratories, Murray Hill, NJ 07974. At the time this article was written he was at the Department of Chemistry, University of North Carolina, Chapel Hill 27514, where R. W. Murray is Kenan Professor of Chemistry.

a source of impetus for the development of the five types of microstructures discussed in this article. These five microstructures—sandwich electrodes, array electrodes, microelectrodes, bilayer electrodes, and ion-gate electrodes—are diagrammed in Fig. 2. The first microstructure to be prepared was the bilayer electrode (Fig. 2, D and E) (*11*), but the sandwich electrode is actually the simplest microstructure and will be discussed first. The emphasis in developing these microstructures has been not only on making microstructures whose electrical behaviors are interesting or potentially useful, but equally on using microstructures as tools to probe the electron and ion transport and other fundamental properties of the constituent electroactive polymers and of their interfaces with one another.

Sandwich Electrodes

The sandwich electrode (Fig. 2A), in which a polymer film is sandwiched between two metallic conductors (*12*), is conceptually the simplest of the microstructures. The electrical conductivity of the polymer, and how it depends on the electrochemical (oxidation) state of the polymer, may be directly measured provided that the sandwich construction allows for supplying or removing the necessary counterions (see reaction 1). In the case (*8*) of several hundred nanometer–thick films of poly[Os(bpy)$_2$(vpy)$_2$](ClO$_4$)$_2$ on platinum electrodes, counterion access is provided through the second electrode, which is a porous gold film that has been evaporated onto the polymer surface. In the case of 10-μm films of polypyrrole on platinum, the second electrode is a solid platinum electrode brought into contact with the film by a sensitive micrometer (*13*). Unless the second platinum electrode is temporarily removed, counterion access becomes constrained to the edges of the film, so that this arrangement is less effective for maintaining electroneutrality during an oxidation state change. These arrangements are shown schematically below.

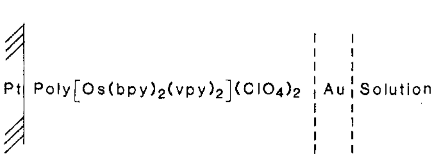

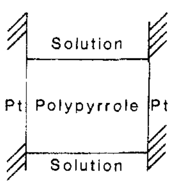

The electrochemical potentials of the two electrodes of either sandwich can be independently controlled with respect to a reference electrode immersed in the contacting electrolyte solution. Applying the same potential (relative to the reference electrode) to both electrodes of the sandwich fixes the oxidation state of the electroactive polymer. The current established between the two connecting electrodes when their potentials (E) are next made slightly different, say, ΔE = 5 mV, gives the conductivity of the polymer at that oxidation state.

Figure 3B shows how the steady-state conductivity of polypyrrole, measured by applying ΔE between the electrodes of a sandwich electrode, varies with the polymer oxidation state. Polypyrrole,

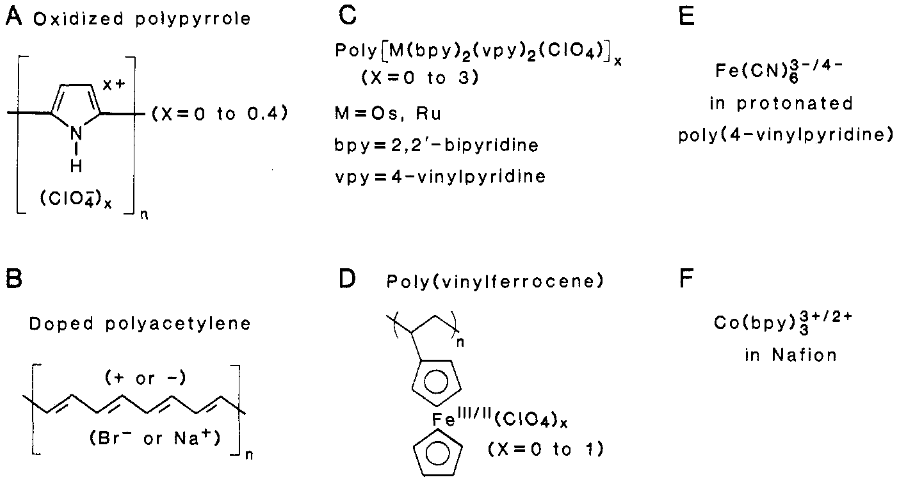

Fig. 1. Types of electroactive polymers. (A and B) The π-conjugated type is electronically conducting and has spatially delocalized electronic states distributed over a broad energy range. (C and D) Redox polymers usually do not have π-conjugation between the electroactive sites, which are electronically localized oxidation-reduction couples covalently bound to the polymer matrix. (E and F) Ion-exchange polymers are conventional polyionic polymers but with mobile redox ions held electrostatically within the polymer matrix. Nafion is a sulfonated fluorocarbon polymer.

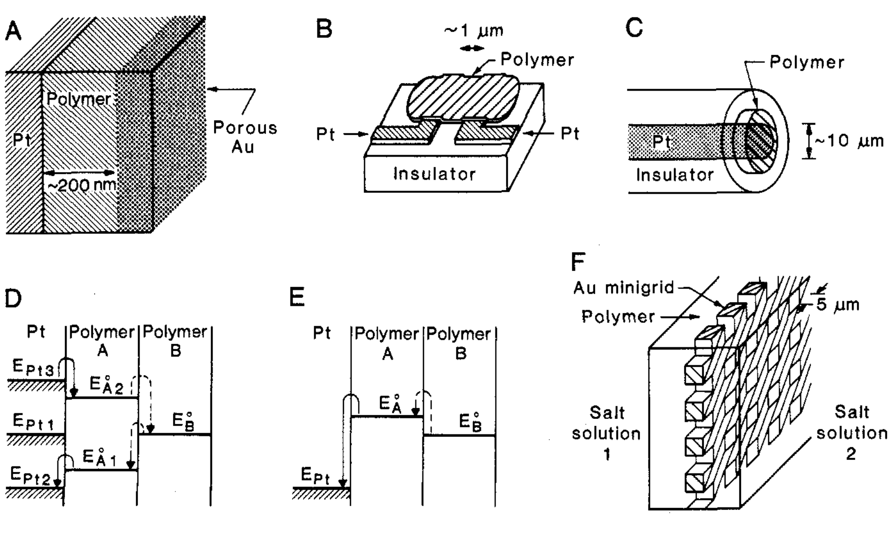

Fig. 2. Microstructures built from electroactive polymers. (A) Sandwich electrode, (B) array electrode, (C) microelectrode, (D) bilayer electrode type 1, (E) bilayer electrode type 2, and (F) ion-gate electrode. Except for (A) and (B), which can also be used in the absence of solvent, an electrolyte solution, reference electrode, and counter electrode are typically present.

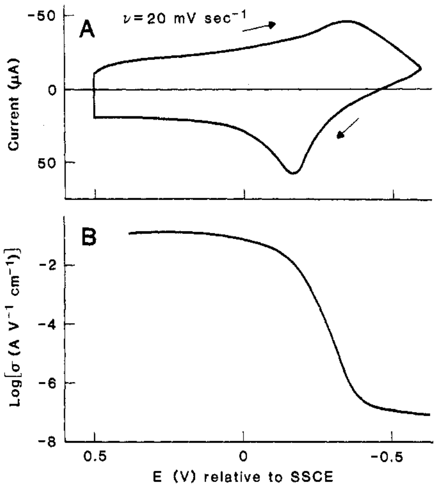

Fig. 3. (A) Cyclic voltammogram and (B) conductivity (σ) of polypyrrole film in contact with 0.1*M* $(C_2H_5)_4NClO_4/CH_3CN$ at room temperature.

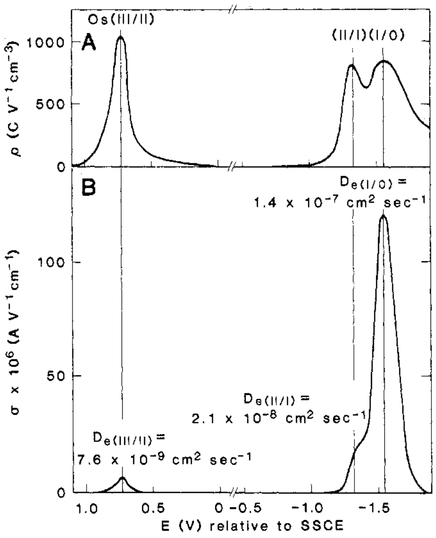

Fig. 4. (A) Redox capacity (ρ) and (B) redox conductivity (σ) of poly$[Os(bpy)_2(vpy)_2](ClO_4)_x$ in contact with 0.1*M* $(C_2H_5)_4NClO_4/CH_3CN$ at room temperature.

when reduced at −0.5 V relative to the sodium chloride–saturated calomel electrode (SSCE) reference electrode, is a poor conductor, but when oxidized at potentials more positive than about −0.1 V compared to SSCE, it is a relatively good conductor (*13, 14*). The cyclic voltammogram of Fig. 3A shows how the electrolysis current into a polypyrrole film (on a simple platinum electrode) varies when the potential is cyclically scanned. Although the hysteresis in the charging current shows that the process is not thermodynamically reversible at the scan rate used, the current-potential curve does demonstrate the capacity of the film to store charge. Comparing A and B in Fig. 3, we see that the considerable oxidative charge that can be stored in polypyrrole at potentials more positive than −0.1 V is not accompanied by further change in the conductivity. The molecular nature of this unusual oxidation remains an active research topic (*13, 15*).

Two additional observations for polypyrrole are (i) that the current through a film of oxidized polymer under a given ΔE is the same whether it is dry or wetted with solvent as in Fig. 3A, and (ii) that the solvent-wetted polymer conducts ohmically up to at least ΔE = 100 mV (that is, current is linear with ΔE over that range). The ohmic behavior is seemingly straightforward evidence (*13*) that the electron flow through the polypyrrole is driven by a voltage gradient in the film between the two electrodes. This ohmic explanation is not unambiguous, however, if one considers the possible consequences of the counterions in the polymer moving appreciably under the influence of the voltage gradient. The counterions, if mobile, will tend to move to eliminate the electric field and, after a long enough time, will accumulate at the interfaces of the metallic electrodes. The applied ΔE, now dropped in part at the two polymer-electrode interfaces, must be accompanied by some oxidation of the polymer at one electrode and reduction at the other. If this occurs, steady-state conduction becomes driven not by the full potential gradient but instead by a concentration gradient of polypyrrole charge carriers. The ohmic experimental result for oxidized polypyrrole implies instead immobility of the counterions and the absence of redox charging due to the imposed bias. The answer to this apparent contradiction is not yet known.

Electron conduction in sandwich electrodes containing poly$[Os(bpy)_2(vpy)_2](ClO_4)_2$ (*8, 16*) is more completely understood. Figure 4A shows the electrochemical capacity ρ of this polymer to store charge plotted as a function of the electrode potential. This plot has the same appearance as a cyclic voltammogram of this polymer, and each of the peaks corresponds to a change of oxidation state. The peaks are centered at the polymer's standard potentials, +0.72, −1.33, and −1.53 V relative to SSCE. Reduction of the Os(III) state of the polymer to Os(II) is primarily a metal-centered reduction, whereas the next two reductions [to the Os(I) and Os(0) forms] are primarily centered on the two bipyridine ligands.

Applying a small ΔE between the two electrodes of the poly$[Os(bpy)_2(vpy)_2](ClO_4)_2$ sandwich and varying their average potential relative to SSCE produces a profile of conductivity, σ, as a function of oxidation state of the polymer film (Fig. 4B). The conductivity plot has features corresponding to each of the capacity peaks in Fig. 4A; that is, conduction occurs when the film is in a mixed valent state. It is only then that electrons on reduced sites can hop to oxidized sites, thereby allowing electron conduction. This self-exchange process between neighboring poly$[Os(bpy)_2(vpy)_2](ClO_4)_x$ sites can be written as

$$\mathrm{Os(III)} + \mathrm{Os(II)} \xrightarrow{k} \mathrm{Os(II)} + \mathrm{Os(III)} \qquad (2)$$

where *K* is the electron self-exchange rate constant. The ClO_4^- counterions migrate within the polymer to eliminate the applied field in the interior of the polymer, so that ΔE is instead dropped at the two polymer-electrode interfaces. The driving force for electron hopping is the concentration gradient of reduced sites. This feature of steady-state electrical conduction in electroactive polymers that contain mobile counterions has led to the term "redox conduction" (*8*). Although redox conductivity can be expressed in the same units as electrical conductivity (amperes per centimeter per volt), redox conduction is driven by electrochemical potential (that is, concentration) gradient, not simply an electric field.

In examining the electrical behavior of polymers like poly$[Os(bpy)_2(vpy)_2](ClO_4)_2$ by means of a transient technique (*17*), it is difficult to determine whether the electrical conductivity is controlled by electron or by counterion mobility, because electrons and counterions are made to migrate concurrently over significant distances through the polymer film as the electrochemical reaction proceeds. In the sandwich electrode, however, the electron flow through the polymer is a steady-state process in which the average polymer oxidation state has been fixed and net counterion migration has ceased. Although counterion motions that are slow over dimensions comparable to site-site separations may still exert some control, the sandwich microstructure allows a more direct measurement of electron mobility for many materials.

If a larger ΔE—say, 200 mV—centered at +0.73 V relative to SSCE [the formal potential of the Os(III)/Os(II) couple] is applied across the poly$[Os(bpy)_2(vpy)_2](ClO_4)_2$ sandwich, all the polymer contacting one electrode becomes oxidized to the Os(III) state and all at the other becomes reduced to Os(II). Figure 5A shows the steady-state concentration-distance profiles of Os(III) and Os(II) sites that develop across the sandwich. The current established is the largest that can be supported by the Os(III/II) mixed valence state of the sandwich. This limiting current (I_{lim}) is given by

$$nFAD_{e(\mathrm{III/II})}\, C_{\mathrm{T}}/d \qquad (3)$$

where F is Faraday's constant, A is the sandwich electrode area, $D_{e(\mathrm{III/II})}$ is the Os(III/II) electron diffusion constant, C_{T} is the total concentration of Os sites (~1.4M), and d is the film thickness. $D_{e(\mathrm{III/II})}$ can be measured on the basis of Eq. 3.

The electron diffusion coefficient D_e is a quantity used to measure the rate of reaction 2, that is, the mobility of charge carriers in polymers such as poly[Os(bpy)$_2$(vpy)$_2$](ClO$_4$)$_2$, in which conduction is driven by concentration gradients. The value of D_e corresponds to the mean squared displacement of the electron per unit time and is given by the ratio, σ:C, of the redox conductivity to electrochemical capacity of the material *(18)*.

Redox conductivity varies with electrochemical potential, as is clearly seen by comparing A and B in Fig. 4. D_e is approximately constant for each particular mixed valence state; that is, we can discuss three different electron diffusion coefficients: $D_{e(\mathrm{III/II})}$, $D_{e(\mathrm{II/I})}$, and $D_{e(\mathrm{I/0})}$. In Fig. 4B, the relative height of each conductivity peak reflects the relative mobility (D_e) of the charge carriers associated with each change of polymer oxidation state. The electrons that reduce the Os(III) complex to the Os(II) complex are about 20 times less mobile than those that reduce the Os(I) complex to the Os(0) complex. Said in more molecular terms, the self-exchange reaction rate constants (k) differ for the Os(III)/Os(II), Os(II)/Os(I), and Os(I)/Os(0) couples, and this gives rise to the different D_e values and redox conductivities shown in Fig. 4B.

Comparing Fig. 3B and Fig. 4B, both of which are normalized for film thickness and electrode area, the electron conductivities of poly[Os(bpy)$_2$(vpy)$_2$](ClO$_4$)$_x$ films are seen to be smaller than the conductivity for polypyrrole, even for the most conductive mixed valence state, Os(I/0). This reflects the difference in electron mobility in a delocalized band material such as polypyrrole and in a material like the osmium polymer, where the electron faces a significant kinetic barrier between each pair of adjacent monomer sites.

We should mention an important recent variant *(19)* of the poly[Os(bpy)$_2$(vpy)$_2$](ClO$_4$)$_2$ sandwich electrode experiment, in which the electrode is not immersed in an electrolyte solution but is instead bathed in a solvent containing no electrolyte (such as toluene or pentane), or in a gaseous medium such as nitrogen with or without solvent vapor, or under vacuum. If we now attempt to generate the situation of Fig. 5A by applying a potential ΔE of 200 mV across the electrodes of the sandwich, no current will be generated. For the steady-state concentration gradients of Fig. 5A to be attained, half the film must become oxidized to the poly[Os(bpy)$_2$(vpy)$_2$](ClO$_4$)$_3$ state. In a solvent-free medium or in a solvent without electrolyte, the extra ClO$_4^-$ counterions necessary to accomplish this oxidation while maintaining overall electroneutrality in the film are simply not available. In other words, there is a restricted ion budget, and conduction will occur only under circumstances not violating it.

Redox conduction can be obtained in the dry sandwich within the ion budget if a much larger ΔE (~2.1 V) is applied. Now, according to the standard potential shown in Fig. 4 [(+0.72 V) − (−1.33 V) = 2.05 V], ΔE is sufficient for simultaneous oxidation and reduction of opposite sides of the film to the Os(III) and Os(I) states, respectively. Electroneutrality and the limited anion budget within the film are satisfied by migration of ClO$_4^-$ anions from the Os(I) side to the Os(III) side. The resulting concentration-distance profiles of Os(III), Os(II), and Os(0) sites are shown in Fig. 5B. The slopes of the concentration profiles are related to the magnitudes of $D_{e(\mathrm{III/II})}$ and $D_{e(\mathrm{II/I})}$, and the populations of Os(III) and Os(I) sites are (to satisfy charge balance) equal. The limiting current for this measurement of electrical conduction across the poly[Os(bpy)$_2$(vpy)$_2$](ClO$_4^-$)$_x$ sandwich reflects the rate of electron self-exchange chemistry in the absence of a bathing electrolyte solution and, in some cases, in the absence of solvent altogether. This experimental capability may have significant fundamental and application utility.

Few examples of polymer sandwich electrodes have been studied so far, partly because of technical limitations in fabricating the microstructure. For instance, the mechanically formed type of sandwich used for polypyrrole is limited to relatively thick films (~10 μm) and is furthermore not optimal for counterion access to the film. The gold evaporation method used to make the poly[Os(bpy)$_2$(vpy)$_2$](ClO$_4$)$_2$ sandwich is useful for much thinner films (0.1 to 0.5 μm), but shorting of the electrodes through minute pinholes in the polymer film can be a problem *(8)*. This problem should be soluble, however, by adapting the reservoir of sophisticated microfabrication strategies accumulated in the microelectronics industry. Preparing the electrode-polymer-electrode sandwich in an open-face sandwich format, as with an array electrode, is one such strategy.

Array Electrodes

The simplest version of this new microstructure arrangement consists of two parallel electrodes separated by a small insulating gap (Fig. 2B). Layering an electroactive polymer film over electrodes and gap as shown in Fig. 2B gives an arrangement formally equivalent to an open-face sandwich electrode. For polymer film thicknesses that are small compared to the width of the gap, the interelectrode gap is equivalent to the sandwich electrode thickness, and the thickness of the polymer film on the array times the length of the parallel electrodes is equivalent to the area of a sandwich electrode film. The area can be large because the electrodes can be folded to form an interdigitated succession called an interdigitated array (IDA).

Wrighton and co-workers *(20, 21)* recently described the first examples of array electrodes coated with electroactive polymers. They prepared arrays with eight independently addressable, parallel gold film electrodes, each 140 μm long and 3 μm wide and separated from one another by 1.4-μm insulating gaps of SiO$_2$. By independent control of the gold electrode potentials, polypyrrole coatings could be electropolymerized onto a single electrode, onto adjacent pairs, or over the entire array. Importantly, the polypyrrole could be made to cover the interelectrode gaps or not, as desired. For the case where two adjacent electrodes and the intervening gap had been coated, the electrical conductivity of polypyrrole in the interelectrode gap was assessed as a function of oxidation state, with results similar to those shown in Fig. 3B.

These results aptly presage the utility of array electrodes in constructing microstructures for both fundamental and device applications. An advantage of array over sandwich electrodes is that the sensitivity of the microstructure to polymer film pinholes and electrode shorting is transferred from the polymer coating step to the array fabrication step, which is based on relatively well-understood microlithographic technology. This means that arrays may be applicable to a larger range of electroactive polymer types than sandwich electrodes to investigate the relation of conductivity to polymer oxidation state. Also, multiple electrodes can be used in varying geometries in the array, several polymer films can be applied to a single array, and ions and chemical reagents may have easier

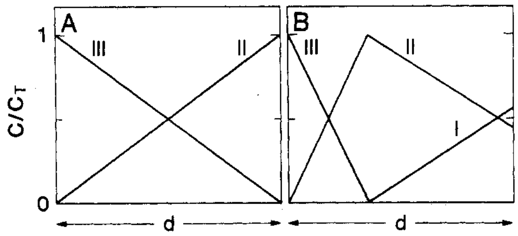

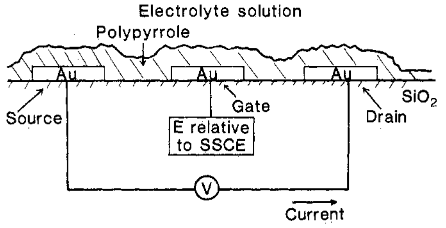

Fig. 5 (left). Concentration-distance profiles of Os(III), Os(II), and Os(I) sites in (A) a platinum–poly[$Os(bpy)_2(vpy)_2](ClO_4)_x$–gold sandwich with ΔE = 200 mV centered about the $E°$ of the Os(III/II) couple ($E_1 \gg E° \gg E_2$) and (B) a dry platinum–poly[$Os(bpy)_2(vpy)_2](ClO_4)_2$–gold film with $\Delta E > 2.1$ V. Fig. 6 (right). An electrochemical transistor based on a polypyrrole coating over a three-terminal gold array electrode (*20*).

access to film structures designed as analytical sensors. Wrighton and co-workers have already illustrated the latter points (*22*).

We have also been interested in array electrodes. Using a 2.5-μm gap IDA made with platinum film electrodes, we have observed (*23*) the redox conduction of poly[$Os(bpy)_2(vpy)_2](ClO_4)_2$ polymers and direct current–electrogenerated chemiluminescence from solutions of the well-studied (*23–25*) complex $[Ru(bpy)_3]^{2+}$. As electrochemists become more familiar with the microlithography required to produce arrays, array electrodes are likely to become a popular base for polymer microstructures. However, whether the array electrode gap will surpass the 0.1-μm gap dimension achievable with sandwich microstructures remains to be seen.

Microelectrodes

The mere fact of being able to shrink the geometrical area of an electrode has great consequences (*26*). For example, the one-terminal, 10-nm disk microelectrode in Fig. 2C has an area of only 8×10^{-7} cm^2. A 100-nm thick poly[$Os(bpy)_2(vpy)_2](ClO_4)_2$ coating on such an electrode contains only about 10^9 monomer sites, which is a tiny quantity in chemical terms (*27*). The currents at the microelectrode are also tiny (down to a few picoamperes), a simple fact that has made solvents with heretofore unusuably low dielectric constants—such as benzene (*28*), toluene, and heptane (*29*)—available for electrochemical experimentation. Such solvents can have profound effects on polymer coatings; for example, electron and counterion mobilities in poly[$Ru(bpy)_2(vpy)_2](ClO_4)_2$ films are 10 to 100 times less in toluene compared to acetonitrile, indicating a stiffened polymer structure due to the tight ion pairing in toluene (*29*). Microelectrode experiments should aid our understanding of the dry sandwich electrode experiments mentioned above.

Polymer-coated microelectrodes are also useful as analytical biosensors because of their small overall physical dimensions. In fact, the concept of microelectrodes at least in part originally developed from a search by Adams and colleagues (*30*) for in vivo electroanalytical probes in neurochemistry. As a recent example, a glassy carbon electrode coated with Nafion polymer films (Fig. 1) has been used in a successful scheme for dopamine neurotransmitter detection (*30*) in rat brain.

Bilayer Electrodes

Bilayer electrodes consist of two different, overlaid electroactive films, one atop the other. The interface between the two films can act as a chemical free-energy–based rectifying junction (*11, 31*). The redox potentials of the polymers selected in designing a bilayer microstructure are crucial; the arrangement shown in Fig. 2D, electrode–polymer *A*–polymer *B*–electrolyte solution, is typical, although important variations from this arrangement are possible.

The principles of bilayer electrodes are straightforward. Because polymer *B* is not in physical contact with the platinum electrode, the platinum electrode can oxidize or reduce polymer *B* states only indirectly and at potentials near the formal potentials $E°_{A1}$ and $E°_{A2}$, where oxidizing and reducing states, respectively, of polymer *A* are generated. For example, a cyclical excursion of the platinum electrode potential from E_{Pt1} to E_{Pt2} and back first oxidizes polymer *A* and thereby polymer *B*, and then re-reduces polymer *A* but does not re-reduce the film of polymer *B*. The current that oxidizes polymer *B* passes the polymer *A*–polymer *B* interface in a rectified manner, leaving polymer *B* charge-trapped in its oxidized state. A secondary event is required to discharge (charge-untrap) polymer *B*; this can occur by raising the electrode potential to E_{Pt3}, resulting in reduction of polymer *B* through the $E°_{A1}$ level of polymer *A*. Polymer *B* could alternatively be reduced through a photolytic reaction, by reaction with a solution component, or by a back reaction (thermodynamically unfavorable and thus slow) with the $E°_{A1}$ level.

The current and charge rectification properties of bilayer microstructures have many possible applications, as will be discussed later. Bilayer electrodes can also be used to probe the polymer film-film interface by measuring the rate at which the monomolecular layer of polymer A sites of the film-film interface exchanges electrons with the opposite monolayer of polymer *B* sites (*32*). The kinetics of such an interfacial process had never been previously explored. A bilayer electrode was constructed (*32*) with redox levels positioned as in Fig. 2E, so that the film-film electron transfer is thermodynamically unfavorable and slow (but not so slow as to be unobservable). With the platinum electrode potential set so that the overall electron transfer from polymer *B* to electrode is favorable, the film-film interfacial electron transfer can become the rate-determining step in bilayer charging. The polymer bilayer electrode used (*32*) was platinum–poly[$Ru(vbpy)_3](ClO_4)_2$–poly[$Os(bpy)_2(vpy)_2](ClO_4)_2$ (vbpy, vinylbipyridine), and the lower limit of the interfacial rate constant for the 405-mV uphill reaction

$$\text{poly}[Os]^{3+} + \text{poly}[Ru]^{2+} \rightarrow \text{poly}[Os]^{2+} + \text{poly}[Ru]^{3+} \quad (4)$$

was found to be within a factor of 30 of that predicted for the self-exchange rates of similar monomer complexes dissolved in solution. Reaction 4 is remarkably fast in view of the many potential chemical and physical barriers that one could readily envision at a polymer-polymer interface. This observation is encouraging for deriving fast switching times in bilayer electrode applications.

Successful functioning of bilayer electrodes depends on making relatively pinhole-free polymer *A* films, and there must be no (or slow) intermingling of the two polymer *A* and *B* films. Bilayers are in fact fairly tolerant of an occasional pinhole, and many combinations (*31*) of different polymers have been made into bilayers with no detectable film-film intermixing effects, at least on the scale of the film thickness.

Bilayer electrodes can be fashioned as sandwich (*33*) and array (*34*) electrodes; for example, as electrode–polymer *A*–polymer *B*–electrode. Such arrangements are useful for electron diffusion studies and also enhance the electrical effects achievable with bilayers.

Ion Gates

The ion gate (Fig. 2F) is a microstructure designed to control the flow of ions rather than of electrons (*35, 36*). A porous electrode is coated with the electroactive polymer to form a freestanding membrane that is used to separate two electrolyte solutions. Its action depends in principle on how the permeability of the electroactive polymer to ion flow changes when, by control of the porous electrode potential, its oxidation state is changed.

The ion gate was first illustrated (*35*) by coating a gold minigrid porous electrode with polypyrrole. Oxidized polypyrrole is polycationic and freely permeable to small anions, whereas the reduced form of polypyrrole is less ionically permeable (by a factor of about 10^2). Thus, by manipulating the potential of the porous gold electrode, the flow of ions through the membrane can be reversibly and repeatedly turned on and off.

Like the other microstructures, the ion gate is useful for fundamental investigations such as, in this case, measuring the ionic conductivity of polypyrrole as a function of oxidation state (*36, 37*) and showing that it parallels the electronic conductivity (Fig. 3A). The ionic conductivity measurement has practical significance as well, since polypyrrole is of interest for charge storage (battery) applications. The ionic conductivity of reduced polypyrrole is so poor that, unless a polypyrrole battery film is designed to facilitate the ingress and egress of counterions, severe ohmic voltage losses will occur during battery charge or discharge.

Toward a Macromolecular Electronics

Macromolecular electronics is not yet a usable reality, but even so, it is possible to state an overall conceptual framework for exploiting the electrical and ionic properties of electroactive polymer microstructures. We make no apology for exploring new concepts that have as yet no technological application, because we have already shown how developing the microstructures has a significant payoff of basic knowledge about electron and ion transport in electroactive polymers. Also, while the polymer microstructures discussed here are based exclusively on electroactive materials, it is possible that the film-making methods being developed will be useful in making thin, nonelectroactive (insulating) polymer films for solid-state electronics.

Bilayer electrode rectification effects: charge trapping. In the bilayer electrode scheme of Fig. 2D, the oxidized form of polymer B can be formed and trapped by changing the electrode potential from E_{Pt1} to E_{Pt2} and back. This trapped, oxidized state amounts to a charge memory (*11, 31*) that can be "read out" by a subsequent potential excursion from E_{Pt1} to E_{Pt3} and back. Further, the bilayer is an accumulating charge memory, because within the redox capacity of polymer B, charge may be summed up over many excursions from E_{Pt1} to E_{Pt2}. The essential difference between charge storage in a bilayer and in a conventional chemical battery is that the bilayer is an astably switched memory element; different potential excursions are necessary for memory input and output. This feature is implicit in all bilayers that have two widely spaced redox levels E°_{A1} and E°_{A2} in the inner (polymer A) film, as in Fig. 2D.

If polymer B has intense colorations that differ from its oxidized and reduced states, then the bilayer is a color memory as well as a charge memory (*38*). This characteristic may be useful in electrochromic displays, which are an active research topic that is close to being a usable technology (*39*). The bilayer configuration would allow astable switching between the color of reduced and oxidized polymer B, which is an important addressing aid in the switching of a multiple-element display. Astable switching of polymeric, electrochromic films can also be accomplished by means of the rectifying characteristics of a semiconductor electrode, as has been recently shown (*40*).

Alternatively, polymer B may react as a sensor of trace reductants or oxidants that diffuse to it from the contacting solution (perhaps a selective sensor by design of its chemistry). The charge stored on reduced or oxidized polymer B can be read out by either trapping or untrapping potential excursions, depending on the chemistry involved. Since the charge is stored cumulatively, great sensitivity is achievable, as illustrated (*38*) by detection of dissolved adventitious oxygen at about $10^{-6}M$.

Bilayer electrode rectification effects: electron-hole pair separation. If illumination of a bilayer electrode produces an excited state of polymer B that is capable of oxidizing polymer A, and if the electrode potential is set so as to re-reduce the oxidized polymer A sites, a cathodic photocurrent will be generated at the electrode. Oyama and co-workers (*41*) have demonstrated this important principle with a bilayer composed of a film of a ruthenium-polypyridine complex covered with a film of a viologen polymer. Use of the chemical free-energy difference at a bilayer film-film interface in this manner is formally analogous to bandgap adsorption and electric field–driven electron-hole pair separation in a semiconductor space-charge region (*42*). Bilayer electrode light-harvesting efficiencies are likely to be less than those of semiconductors, however, unless polymers or modified microstructures can be identified that allow substantial exciton migration (or the equivalent), and where the back electron transfer reactions regenerating the original ground-state reactants are slow. Also, to prevent the film of polymer B from gradually becoming completely reduced, the contacting solution must contain a chemical oxidant, or a second electrode must be provided to act as an electron acceptor, as in the sandwich or array electrodes. Oyama and co-workers (*41*) used dissolved dioxygen as the oxidant; the effect was to regenerate viologen (polymer B) and also partially quench the ground-state back reaction of reduced viologen with the Ru(III) polymer.

Current-potential characteristics: two-electrode structures and electrochemical diodes. That the current through the electroactive polymer film in a sandwich electrode or on an array varies with interelectrode potential in a nonlinear fashion has been pointed out by both Wrighton's laboratory (*21*) and our own (*33*). There is little current between the electrodes unless their potential difference exceeds a certain value, whereupon a steep increase in current occurs, much like a Zener diode breakdown voltage.

The specifics of the electrochemical diode depend on several factors, but particularly upon the choice of electroactive polymer. For instance, the voltage of the rapid current rise for a poly[Os$(\mathrm{bpy})_2(\mathrm{vpy})_2](\mathrm{ClO_4})_2$ sandwich electrode in electrolyte solution depends on the potentials of the two electrodes relative to some reference electrode (*33*), but when used in vacuum (*19*) current starts at a characteristic value near $E^\circ_{3/2}$ to $E^\circ_{2/1}$. In both media, the current does not increase indefinitely but reaches a plateau when the limiting concentration gradient conditions shown in Fig. 5, A or B, are attained. An electrochemical diode made from an array coated with polypyrrole (*21*) has a current-voltage characteristic more like a conventional *p-n* junction diode, but the initial voltage can be varied systematically by choice of the reference electrode potential. Use of polyaniline, a different conducting polymer, on the array (*22*) produces an unusual diode pattern; after an initial voltage breakdown, the current reaches a plateau and then, at a larger interelectrode voltage, returns to a small value. This novel diode characteristic occurs because the conductive form of polyaniline can be made insulating by either oxidizing or reducing it further. Diodes can also be based on polymer bilayers incorporated into sandwich (*33*) or array (*34*) electrodes.

The range of different current-potential characteristics may ultimately lead to interesting uses for electrochemical diodes based on microstructured polymers. It is unlikely, however, that these electrochemical diodes will compete with the switching speed of solid-state devices. The intrinsically slow transport of electrons and ions required to turn on electrochemical diodes may, on the other hand, be ameliorated considerably if the macromolecular dimensions of the electrochemical diode can be shrunk to molecular dimensions, since this shortens the transport distances.

Electrochemical diodes can emit light if the oxidized and reduced members of two different redox couples, generated at opposite faces of a sandwich electrode (or adjacent electrodes in an array), react energetically enough to produce luminescing, excited-state species. This principle has not yet been demonstrated with electroactive polymers, but Bard and Brilmyer (*43*) have described the solution analog using a variety of dissolved redox couples in a twin-electrode thin-layer cell.

Amplification with three electrode structures: electrochemical transistors and triodes. These microstructures indirectly control the current between two electrodes contacting an electroactive polymer by controlling the potential applied to a third electrode. Two different microstructures have been reported that accomplish this (*20, 33*). One, labeled a "triode" (*33*), was based on the poly[Os(bpy)$_2$(vpy)$_2$](ClO$_4$)$_2$ sandwich electrode with an external reference electrode as the third electrode carrying the input signal. The other, labeled a "transistor" (*20*), was based on a three-electrode polypyrrole array scheme as shown in Fig. 6. In this scheme, the gate electrode, whose potential is controlled at E relative to an SSCE reference electrode in the contacting solution, is capable of generating a strip of polypyrrole of widely varying conductivity that is interposed between the source and drain electrodes. As a consequence, the current between the source and drain electrodes under the impetus of a constant impressed potential (V) is sensitive to the potential (E) applied to the gate electrode. The significant feature is that the effect of the gate potential is greatly amplified; a tiny charge flowing to the gate has a large impact on the drain current.

Although practical application will require substantial advances, the achievement (*20*) of amplification by this arrangement is an important conceptual step toward a macromolecular electronics. Amplifying signals that are based on chemical events is difficult and has usually been sought through catalytic reactions. The gate electrode described above could be replaced or controlled by an analyte-sensing reaction (*22*), so that the amplification demonstrated in the Wrighton experiment is also an attractive concept for novel, sensitive analytical sensors that are based on polymer-coated arrays.

Ionic effects. Since the ion gate is a remotely, electrically switchable membrane, it offers an "on-off" avenue for control of ion transport from one medium to another. Release of ionic reagents is one possible application, and Miller and Zinger (*44*) have exploited this by soaking polypyrrole films in glutamate solutions, which introduces this anion into the films as a counterion. Reducing the polypyrrole film then releases the glutamate into the contacting solution in small but controllable doses. In a microelectrode format, such a device could be valuable in neurochemical research.

Conclusions

Although macromolecular electronics is still at a rudimentary level, the concepts involved are quite novel and with continued development may lead to practical applications. In fact, the concepts have on a number of occasions in our own research outrun the availability of suitable polymeric redox materials or our ability to fabricate a suitable microstructure from a polymer. A high priority in this field, for those interested in practical applications, will be development of a wider variety of robust, well-behaved electroactive materials to be used in the microstructures. Given the fast pace of development of electroactive polymer films since the seminal reports of polymer film electroactivity (*45*), many of the materials' limitations may gradually be solved.

REFERENCES AND NOTES

1. R. W. Murray, *Annu. Rev. Mater. Sci.* **14**, 145 (1984); in *Electroanalytical Chemistry*, A. J. Bard, Ed. (Dekker, New York, 1984), vol. 13, p. 191.
2. R. B. Seymour, Ed., *Conductive Polymers* (Plenum, New York, 1981); T. Skotheim, Ed., *Handbook of Conducting Polymers* (Dekker, New York, in press).
3. P. Pfluger, M. Krounbi, G. B. Street, G. Weiser, *J. Chem. Phys.* **78**, 3212 (1983).
4. A. G. MacDiarmid and A. J. Heeger, *Syn. Metals* **1**, 101 (1979).
5. N. S. Murthy, R. H. Elsenbaumer, J. E. Frommer, R. H. Baughman, *ibid.* **9**, 91 (1984).
6. A. F. Diaz, K. K. Kanazawa, G. P. Gardini, *J. Chem. Soc. Chem. Commun.* (1979), p. 635.
7. G. Tourillon and F. Garnier, *J. Phys. Chem.* **87**, 2289 (1983).
8. P. G. Pickup, W. Kutner, C. R. Leidner, R. W. Murray, *J. Am. Chem. Soc.* **106**, 1991 (1984).
9. P. Denisevich, H. D. Abruna, C. R. Leidner, T. J. Meyer, R. W. Murray, *Inorg. Chem.* **21**, 2153 (1982); P. J. Peerce and A. J. Bard, *J. Electroanal. Chem.* **114**, 89 (1980); F. B. Kaufman, A. H. Schroeder, E. M. Engler, S. R. Kramer, J. Q. Chambers, *J. Am. Chem. Soc.* **102**, 483 (1980); J. B. Kerr, L. L. Miller, M. R. Van De Mark, *ibid.*, p. 3383.
10. N. Oyama, S. Yamaguchi, Y. Nishiki, K. Tokuda, H. Matsuda, F. C. Anson, *J. Electroanal. Chem.* **139**, 371 (1982); D. A. Buttry and F. C. Anson, *J. Am. Chem. Soc.* **105**, 685 (1983).
11. H. D. Abruna, P. Denisevich, M. Umana, T. J. Meyer, R. W. Murray, *J. Am. Chem. Soc.* **103**, 1 (1981).
12. P. G. Pickup and R. W. Murray, *ibid.* **105**, 4510 (1983).
13. B. J. Feldman, P. Burgmayer, R. W. Murray, *ibid.* **107**, 872 (1985).
14. K. K. Kanazawa *et al.*, *J. Chem. Soc. Chem. Commun.* (1979), p. 854.
15. S. W. Feldberg, *J. Am. Chem. Soc.* **106**, 4671 (1984); G. Wegner, *Mol. Cryst. Liq. Cryst.* **106**, 269 (1984); K. Yakushi, L. J. Lauchlan, T. C. Clarke, G. B. Street, *J. Chem. Phys.* **79**, 4474 (1983).
16. C. E. D. Chidsey and R. W. Murray, in preparation; C. R. Leidner and R. W. Murray, *J. Am. Chem. Soc.* **106**, 1606 (1984).
17. J. S. Facci, R. H. Schmehl, R. W. Murray, *ibid.* **104**, 4959 (1982).
18. While all the elements are present in earlier work [see especially (*8*)], we only recently recognized this simple relation, which is exactly valid for those cases where conduction is driven entirely by concentration gradients (C. E. D. Chidsey and R. W. Murray, *J. Phys. Chem.*, in press).
19. J. C. Jernigan, C. E. D. Chidsey, R. W. Murray, *J. Am. Chem. Soc.* **107**, 2824 (1985).
20. H. S. White, G. P. Kittlesen, M. S. Wrighton, *ibid.* **106**, 5375 (1984).
21. G. P. Kittlesen, H. S. White, M. S. Wrighton, *ibid.*, p. 7389.
22. E. W. Paul, A. J. Ricco, M. S. Wrighton, *J. Phys. Chem.* **89**, 1441 (1985).
23. C. E. D. Chidsey, B. J. Feldman, C. Lundgren, R. W. Murray, in preparation.
24. J. D. Luttmer and A. J. Bard, *J. Phys. Chem.* **85**, 1155 (1981).
25. R. S. Glass and L. R. Faulkner, *ibid.*, p. 1160.
26. J. O. Howell and R. M. Wightman, *Anal. Chem.* **56**, 524 (1984).
27. A. G. Ewing, B. J. Feldman, R. W. Murray, *J. Electroanal. Chem.* **172**, 145 (1984).
28. J. O. Howell and R. W. Wightman, *J. Phys. Chem.* **88**, 3915 (1984).
29. L. Geng, A. E. Ewing, J. C. Jernigan, R. W. Murray, in preparation.
30. J. A. Gerhardt, A. F. Oke, J. Nagy, B. Moghaddam, R. N. Adams, *Brain Res.* **290**, 390 (1983).
31. P. Denisevich, K. W. Willman, R. W. Murray, *J. Am. Chem. Soc.* **103**, 4727 (1981).
32. C. R. Leidner and R. W. Murray, *ibid.* **107**, 551 (1985).
33. P. G. Pickup and R. W. Murray, *J. Electrochem. Soc.* **131**, 833 (1984).
34. J. P. Kittlesen, H. S. White, M. S. Wrighton, preprint (1985).
35. P. Burgmayer and R. W. Murray, *J. Electroanal. Chem.* **147**, 339 (1983).
36. ———, *J. Phys. Chem.* **88**, 2515 (1984).
37. ———, in *Handbook of Conducting Polymers* (Dekker, New York, in press).
38. K. W. Willman and R. W. Murray, *J. Electroanal. Chem.* **133**, 211 (1982).
39. M. M. Nicholson, *Ind. Eng. Chem. Prod. Res. Dev.* **21**, 261 (1982).
40. O. Inganas and I. Lundstrom, *J. Electrochem. Soc.* **131**, 1129 (1984).
41. N. Oyama, S. Yamaguchi, M. Kaneko, A. Yamada, *J. Electroanal. Chem.* **139**, 215 (1982).
42. H. Gerischer, *ibid.* **58**, 263 (1975).
43. G. H. Brilmyer and A. J. Bard, *J. Electrochem. Soc.* **127**, 104 (1980).
44. B. Zinger and L. L. Miller, *J. Am. Chem. Soc.* **106**, 6861 (1984).
45. M. S. Wrighton, M. C. Palazzotto, A. B. Bocarsly, J. M. Bolts, A. B. Fischer, L. Nadjo, *ibid.* **100**, 7264 (1978); A. Merz and A. J. Bard, *ibid.*, p. 3222; M. R. Van De Mark and L. L. Miller, *ibid.*, p. 3223; R. Nowak, F. A. Schultz, M. Umana, H. Abruna, R. W. Murray, *J. Electroanal. Chem.* **94**, 219 (1978).
46. Our research in fabrication and fundamentals of polymer microstructures has been supported by NSF, Chevron, and the Office of Naval Research.